[Chem. Pharm. Bull. 24(1) 61—71 (1976)]

UDC 547.775.02.03 : 543.422.25

^{13}C Nuclear Magnetic Resonance Spectra of Antipyrine Derivatives and Their Application to Hansch Analysis

Jutaro Okada, Toshiyuki Esaki,[1a] and Kunimi Fujieda[1b]

Faculty of Pharmaceutical Sciences, Kyoto University[1a] and Naka Works, Hitachi, Ltd.[1b]

(Received May 13, 1975)

The ^{13}C nuclear magnetic resonance spectra of thirty 4-substituted antipyrine derivatives were examined to obtain the following conclusions: (i) the shielding constants of antipyrine were estimated using the CNDO/2 method; the signal assignment using the shielding constants was consistent with that based on the experiments; (ii) the ^{13}C–^{1}H coupling constants of antipyrine were estimated using the CNDO/2 method; the calculated values are in good agreement with those observed; (iii) the additive equation on the chemical shifts of the sp^3-hybridized carbon was estimated; the so-called steric effects were observed as a result of this analysis; and (iv) the Hansch analyses were carried out regarding C-4 of the antipyrine derivatives as the so-called biological active center; the agreement between the values estimated by the Hansch equation and those observed was fairly good for the analgesic activities.

Since antipyrine which Knorr synthesized at the outset in 1884 was found to have antipyretic and analgesic activities, a number of its 4-substituted derivatives have been synthesized for inventing new antipyretics or analgesics. In this paper, ^{13}C nuclear magnetic resonance (^{13}C NMR) spectra of thirty 4-substituted derivatives including aminopyrine, isopropylantipyrine, aminopropylon, sulpyrine, and nicotinoylantipyrine, which at present are widely used, have been examined and discussed. Further, the Hansch analysis using ^{13}C chemical shifts has been carried out regarding C-4 of the antipyrine derivatives as the so-called biological active center.[2]

Result of Measurement

The ^{13}C chemical shifts, δ_c, of the thirty derivatives are tabulated in Table I. As an example, the natural abundance ^{1}H-noise-decoupled ^{13}C NMR FT spectrum of antipyrine is shown in Fig. 1.

The ^{13}C signals of antipyrine were assigned using the technique of an off-resonance decoupling and lanthanide-induced shift measurements[3] with a shift reagent $Pr(fod)_3$. By the off-resonance decoupling, the signals at δ 12.9 and 35.7 were split into quartets, those at δ 96.4, 123.5, 125.8, and 128.7 into doublet, and those at δ 135.0, 157.1, and 164.8 remained singlets. Remaining assignments were based on the $Pr(fod)_3$-induced shifts, which were simply assumed to follow McConnell-Robertson's equation. The orders of magnitudes of the induced shifts were observed as follows: C-5>C-1′>C-3 for the singlets, C-4>C-2′—C-6′>C-3′—C-5′>C-4′ for the doublets, and N–CH_3>C–CH_3 for the quartets. The induced shifts for a solution with a 1:1 Pr-antipyrine mole ratio are summarized in Table II. Figure 2 shows the induced shift changes when $Pr(fod)_3$ was added by degrees in 0.1 mole fractions. Thus, the ^{13}C signals

1) Location: *a) Yoshida-Shimoadachi-cho, Sakyo-ku, Kyoto; b) 882, Ichige, Katsuta, Ibaraki.*
2) J. Okada and T. Esaki, *Chem. Pharm. Bull.* (Tokyo), **22**, 1580 (1974).
3) G.C. Levy and G.L. Nelson, "Carbon-13 Nuclear Magnetic Resonance for Organic Chemists," John Wiley and Sons, Inc., New York, N.Y., 1972, p. 24.

TABLE I. ^{13}C Chemical Shifts of Antipyrine Derivatives, δ_C

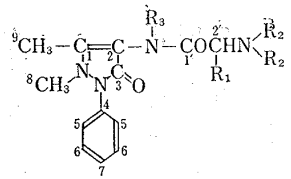

No.1—No.12

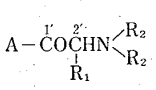

No.13—No.18

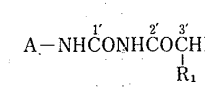

No.19—No.21

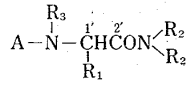

No.22—No.24

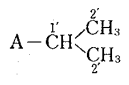

No.26

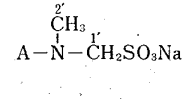

No.27

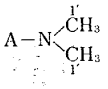

No.28

No.29

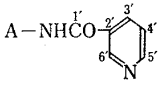

No.30

No.	R_1	R_2	R_3	C-1	C-2	C-3	C-4	C-5	C-6	C-7	C-8	C-9	C-1′	C-2′	C-3′	R_1 C-1	R_1 C-2	R_1 C-3	R_2 C-1	R_2 C-2	R_3 C-1	Solvent
1	H	CH_3	H	151.1	107.0	160.9	134.5	122.9	128.5	125.7	36.1	11.3	168.2	62.1					45.2			DMSO
2	H	C_2H_5	H	150.0	107.1	160.4	134.1	122.4	128.0	125.1	36.0	11.3	169.0	56.5					47.5	12.0		DMSO
3	CH_3	CH_3	H	150.4	106.9	160.2	134.0	122.4	128.0	125.1	35.9	11.1	170.4	62.8		12.4			(40.4)[a]			DMSO
4	CH_3	C_2H_5	H	149.9	107.9	160.4	134.5	122.7	128.3	125.5	36.0	11.2	171.8	58.6		10.4			43.7	13.1		DMSO
5	C_2H_5	CH_3	H	150.5	106.9	160.1	134.0	122.5	128.0	125.2	35.8	11.1	169.0	68.8		21.7	10.2		(40.2)			DMSO
6	C_2H_5	C_2H_5	H	150.8	107.6	160.8	134.3	122.5	128.1	125.1	36.0	11.3	170.9	64.9		21.4	11.3		43.5	13.8		DMSO
7	C_3H_7	CH_3	H	151.2	107.7	160.9	134.6	122.9	128.5	125.6	36.2	11.5	169.9	67.1		31.1	19.2	14.1	(40.8)			DMSO
8	C_3H_7	C_2H_5	H	150.7	108.0	160.9	134.6	122.9	128.5	125.5	36.2	11.5	171.1	63.0		30.5	19.9	14.1	44.0	14.1		DMSO
9	CH_3	CH_3	CH_3	150.2	112.2	159.0	132.1	121.9	126.8	124.6	35.2	10.5	171.1	58.3		10.5			40.3		35.2	$CHCl_3$
10	CH_3	C_2H_5	CH_3	149.9	112.8	158.7	132.1	121.9	126.9	124.5	36.0	11.0	171.7	54.3		9.5			43.2	13.9	35.4	$CHCl_3$
11	C_2H_5	CH_3	CH_3	150.3	112.3	158.6	132.2	121.7	126.7	124.3	35.3	10.9	170.1	64.5		17.6	10.9		40.4		35.3	$CHCl_3$
12	C_3H_7	CH_3	CH_3	150.6	112.6	159.1	132.6	122.0	127.0	124.8	35.6	10.9	170.6	62.8		26.2	19.7	14.1	40.7		35.6	$CHCl_3$
13	H	CH_3	—	154.1	103.3	162.0	133.1	126.1	128.6	127.5	33.3	11.9	191.0	65.9					45.3			DMSO
14	CH_3	CH_3	—	154.5	103.7	161.8	133.1	126.0	128.5	127.2	33.2	11.9	194.6	61.0		10.8			(40.4)			DMSO
15	CH_3	C_2H_5	—	154.7	103.6	161.8	133.4	126.0	128.6	127.3	33.3	11.8	196.5	58.6		12.8			44.0	14.3		DMSO
16	C_2H_5	CH_3	—	154.1	104.3	161.9	133.1	126.0	128.4	127.2	33.3	12.0	194.3	66.4		18.9	10.7		(40.4)			DMSO
17	C_2H_5	C_2H_5	—	154.1	104.1	161.9	133.3	126.0	128.3	127.2	33.4	11.7	196.3	64.1		20.3	10.9		43.9	14.4		DMSO
18	iso-C_3H_7	CH_3	—	154.0	105.9	162.7	133.5	126.2	128.6	127.4	33.4	12.1	194.7	69.9		26.3	19.6		(40.7)			DMSO
19	H	$N(CH_3)_2$	—	148.0	105.6	158.8	132.3	121.7	126.7	124.2	35.6	11.5	148.7	168.9	61.6				45.0			$CHCl_3$
20	CH_3	$N(CH_3)_2$	—	147.7	105.9	158.5	132.4	121.8	126.6	124.2	35.5	11.1	148.7	172.0	63.2	9.5			41.1			$CHCl_3$
21	iso-C_3H_7	Br	—	147.9	102.5	159.0	131.5	125.6	128.0	128.0	34.3	10.8	152.5	168.3	55.7	32.2	20.0					CD_3COOD Ext. TMS
22	H	H	H	142.5	115.3	159.2	131.5	124.3	127.5	126.4	34.8	9.9	50.6	174.7								CD_3COOD Ext. TMS
23	CH_3	CH_3	H	138.9	115.5	158.9	132.9	120.9	126.7	123.5	35.1	9.9	48.8	171.4		19.0			{36.2 37.1			$CHCl_3$
24	CH_3	CH_3	CH_3	148.5	118.9	160.6	132.7	121.3	126.7	123.9	35.1	10.3	55.7	169.4		14.5			{36.0 36.6		38.0	$CHCl_3$
25	Antipyrine			157.1	96.4	164.8	135.0	123.5	128.7	125.8	35.7	12.9										DMSO
26	Isopropylantipyrine			149.6	114.0	162.5	133.3	121.0	126.6	123.4	36.1	11.1	24.2	21.1								$CDCl_3$
27	Sulpyrine			149.1	117.4	160.9	132.1	125.9	128.7	128.1	35.0	11.5	72.6	43.8								D_2O
28	Aminopyrine			149.6	121.5	161.7	134.4	122.1	128.0	124.9	36.3	10.0	43.3									DMSO
29	Antipyrylurea			148.0	103.5	158.7	131.4	125.6	127.9	127.9	34.1	10.2	173.7			C-4′ 123.3	C-5′ 147.3	C-6′ 144.7				CD_3COOD Ext. TMS
30	Nicotinoylantipyrine			147.9	103.4	158.5	131.4	125.6	127.9	127.9	34.4	10.9	163.0	128.5	136.1							CD_3COOD Ext. TMS

a) The parenthesized figures are estimated values.

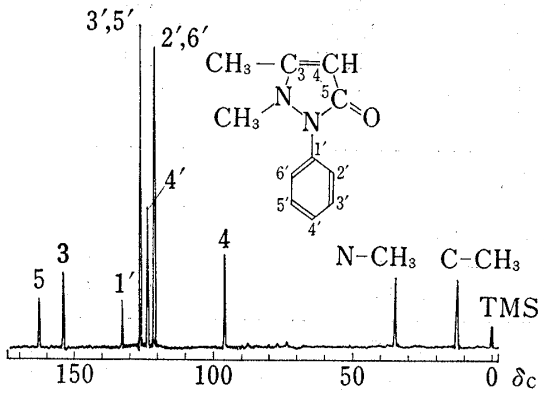

Fig. 1. The Natural-abundance ^{1}H-noise-decoupled ^{13}C PFT NMR Spectrum of Antipyrine in $CDCl_3$

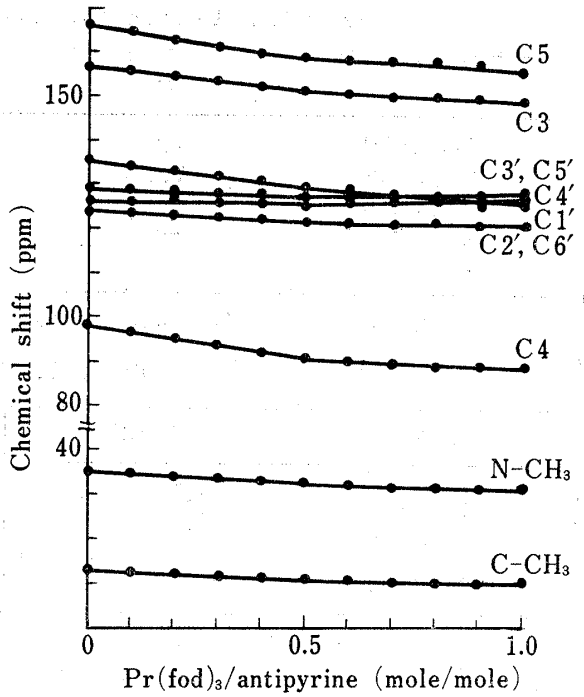

Fig. 2. A Plot of Chemical Shifts of Antipyrine at Several Concentrations of Added $Pr(fod)_3$

TABLE II. $Pr(fod)_3$-Induced Shifts (1: 1 Mole Ratio of $Pr(fod)_3$: Antipyrine)

Position	Δ (ppm)	Position	Δ (ppm)
3	−8.2	1′	−10.2
4	−10.1	2′, 6′	−3.6
5	−11.6	3′, 5′	−2.0
N-CH_3	−4.4	4′	0.3
C-CH_3	−2.7		

of antipyrine were assigned as shown in Fig. 1, and those of the other derivatives examined were assigned with comparison from compound to compound.

Theoretical Calculation[4]

Theoretical calculations of the shielding constants and the spin coupling constants for antipyrine were carried out using the CNDO/2 method. Table III lists the parameter values used in the calculations. The Cartesian coordinates of the constituent atoms are also necessary. The coordinates of the constituent atoms were determined by means of constructing an ideal molecular model using the bond lengths in Table IV. According to the results of an X-ray analysis, [5a] the actual structure of antipyrine is visualized as a resonance hybrid somewhere between the following three extremes. But structure (I) was only calculated for convenience. The conformational change owing to the free rotation around the single bond between N-1 and C-1′ is in this case thought to influence greatly on the electronic state of the antipyrine molecule. The total energy variation owing to the free rotations, which was calculated using the EHT method, is presented in Fig. 3, which shows that the total energy

4) The calculations were performed on a Facom 230—75 computer of the Data Processing Center, Kyoto University.

5) *a*) M. Vijayan and M.A. Viswamitra, *Acta Cryst.*, **24B**, 1067 (1968); *b*) M. Vijayan, *Curr. Sci.*, **40**, 489 (1971).

Table III. Parameter Values used for CNDO/2 Calculations[a)]

	H	C	N	O
$\zeta\ (=Z^*/n^*)$	1.20	1.625	1.95	2.275
$(I_s+A_s)/2$	7.176	14.051	19.316	25.390
$(I_p+A_p)/2$	—	5.572	7.275	9.111
β_A	−9	−21	−25	−31
Z	1	4	5	6

a) J.A. Pople and G.A. Segal, *J. Chem. Phys.*, **44**, 3289 (1966)

Table IV. Bond Length

Bond	Length (Å)	Bond	Length (Å)
C-C	1.54	C=O	1.22
C=C	1.35	C-N	1.47
C=C (Benzene)	1.40	N-N	1.45
		C-H	1.09

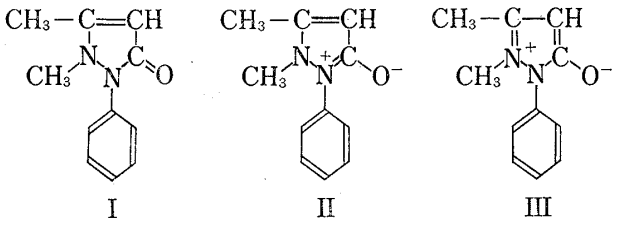

I II III

is minimized when the pyrazolone ring and the phenyl ring are tilted with respect to each other by *ca.* 60°. Therefore, the electronic state of antipyrine was calculated for convenience with the angle of 60° in the following considerations. By the way, the angle between an average molecular plane of the pyrazolone ring and that of the phenyl ring is *ca.* 24° according to the result of calculations using the X-ray data.[5b)] Figure 4 shows the charge distribution of antipyrine obtained by the CNDO/2 calculation.

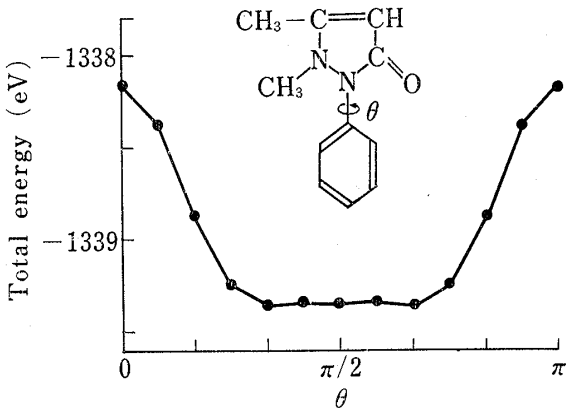

Fig. 3. Variation in Total Energy by Rotation around N_1–C_1' Axis of Antipyrine

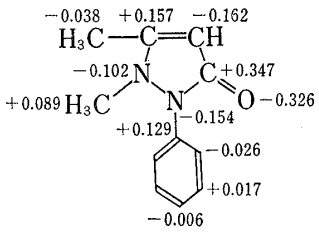

Fig. 4. Electron Distribution in Antipyrine

Consideration

Shielding Constant[6)]

The shielding constant is generally expressed as Eq. (1);

$$\sigma^A = \sigma_d{}^A + \sigma_p{}^A \quad (1)$$

6) J. Okada and T. Esaki, *Yakugaku Zasshi*, **95**, 56 (1975).

where σ_d^A denotes the diamagnetic term and σ_p^A denotes the paramagnetic term. Assuming that the equation $\sigma_d^A = 4.45Z^*q^A$ (Z^*: effective nuclear charge, q^A: total electron density) can apply, the contribution of the σ_d^A term to the total shielding constant σ^A is 4.3 ppm (54.8—59.1 ppm), which is *ca.* 3% of the total chemical shift range of 151.9 ppm (12.9—164.8 ppm). Therefore, the σ_d^A term was neglected in the following calculations. Table V lists the intermediate data which were necessary in the calculations.

TABLE V. Calculations of Shielding Constants

Position	$\langle r^{-3}\rangle_{2p}$	$\sum_B Q_{AB}$	$-\sigma_p^A$	$\delta^{13}C_{calcd.}$	$\delta^{13}C_{obsd.}$
3	1.512	2.609	362.5	149.1	157.1
4	1.371	2.459	309.8	96.4	96.4
5	1.618	2.608	387.8	174.4	164.8
N–CH_3	1.484	2.132	242.4	29.0	35.7
C–CH_3	1.424	2.137	233.1	19.7	12.9
1′	1.488	2.624	358.9	145.5	135.0
2′, 6′	1.425	2.513	329.0	115.6	123.5
3′, 5′	1.442	2.522	334.2	120.8	128.7
4′	1.432	2.520	331.7	118.3	125.8

The results are given in Eq. (2) for the sp^3-carbon, in Eq. (3) for the sp^2-carbon.

$$sp^3\text{-carbon: } \sigma^A \fallingdotseq \sigma_p^A = -76.6\langle r^{-3}\rangle_{2p}\sum_B Q_{AB} \quad (2)$$

$$sp^2\text{-carbon: } \sigma^A \fallingdotseq \sigma_p^A = -91.9\langle r^{-3}\rangle_{2p}\sum_B Q_{AB} \quad (3)$$

The average excitation energies (ΔE) were estimated at 9.51 eV for the sp^3-carbon and at 7.93 eV for the sp^2-carbon by taking $(e\hbar/mc)^2$ as 53.2×10^{-6}. The values estimated by Eq. (5) and (6) are plotted against the observed values in Fig. 5, which shows that the signal assignment using the shielding constants is consistent with that based on the experiments. In addition, the total electron densities are also plotted against the observed values in Fig. 5, which shows that the order of the total electron densities corresponds to that of the chemical shifts in the range of the sp^2-carbon.

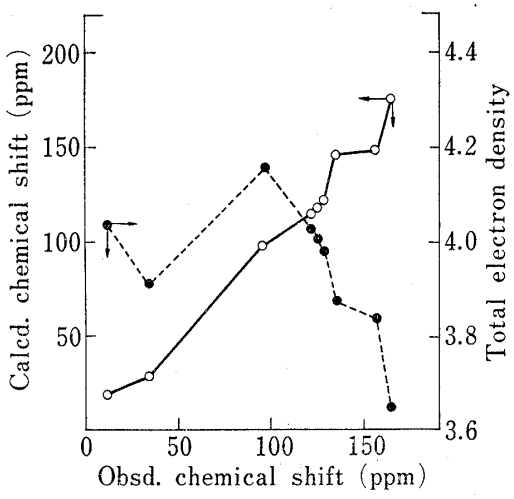

Fig. 5. Plots of Calcd. Chemical Shift and Total Electron Density *versus* Obsd. Chemical Shift

Coupling Constant[7]

The coupling constant between the nuclei C and H is conveniently expressed as Eq. (4);

$$J_{C\text{-}H} = J_{C\text{-}H}^{(1a)} + J_{C\text{-}H}^{(1b)} + J_{C\text{-}H}^{(2)} + J_{C\text{-}H}^{(3)} \quad (4)$$

where $J_{C\text{-}H}^{(1a)}$ and $J_{C\text{-}H}^{(1b)}$ are the orbital terms, $J_{C\text{-}H}^{(2)}$ is the spin dipolar term and $J_{C\text{-}H}^{(3)}$ is the Fermi interaction term. In general, the $J_{C\text{-}H}^{(3)}$ term dominantly contributes to $J_{C\text{-}H}$, and the $J_{C\text{-}H}^{(1a)}$, the $J_{C\text{-}H}^{(1b)}$ and the $J_{C\text{-}H}^{(2)}$ terms can be neglected as an approximation. According to the molecular orbital theory, $J_{C\text{-}H}^{(3)}$ is given in Eq. (5);

$$J_{C\text{-}H}^{(3)} = -(\hbar/2\pi)(256\pi^2/9)\gamma_C\gamma_H\beta^2(S_C|\delta(\mathbf{r}_C)|S_C)(S_H|\delta(\mathbf{r}_H)|S_H) \times \sum_i^{occ.}\sum_j^{unocc.}({}^3\Delta E_{i\to j})^{-1}C_{is_C}C_{js_C}C_{js_H}C_{is_H} \quad (5)$$

7) *a*) T. Yonezawa, C. Nagata, H. Kato, A. Imamura, and K. Morokuma, "Ryosi Kagaku Nyumon (Ge)," revised ed., Kagaku Dojin, Kyoto, 1969, pp. 602—612; *b*) T. Yonezawa, I. Morishima, and M. Fujii, *Bull. Chem. Soc., Japan*, **39**, 2110 (1966); *c*) T. Yonezawa, I. Morishima, M. Fujii, and H. Kato, *ibid.*, **42**, 1248 (1969).

By using the mutual polarizability $\pi_{s_Cs_H}$, Eq. (5) is rewritten to Eq. (6);

$$J^{(3)}_{C-H} = -(\hbar/2\pi)(64\pi^2/9)\gamma_C\gamma_H\beta^2 S_C^2(0)S_H^2(0)\pi_{s_Cs_H} \quad (6)$$

where $S_C^2(0)$ and $S_H^2(0)$ represent the magnitudes of the valence s orbitals at the nuclei C and H. The values of $S_C^2(0)$ and $S_H^2(0)$, which are obtained using the Slater AO for H atom and using the Hartree-Fock SCF AO for C atom, are 2.768 and 0.5500 (a.u.), respectively; $\pi_{s_Cs_H}$ denotes the mutual polarizability of the valence s orbitals belonging to C and H atoms, defined as Eq. (7).

$$\pi_{s_Cs_H} = 4\sum_i^{occ.}\sum_j^{unocc.}(\varepsilon_i-\varepsilon_j)^{-1}C_{is_C}C_{is_H}C_{js_C}C_{js_H} \quad (7)$$

By adopting the mean exitation energy approximation ($^3\Delta E$) instead of $^3\Delta E_{i\to j}$ and by using the relation $\sum_i^{occ.}C_{is_C}C_{is_H} = -\sum_j^{unocc.}C_{js_C}C_{js_H}$, Eq. (5) is also rewritten to Eq. (8).

$$J^{(3)}_{C-H} = (\hbar/2\pi)(64\pi^2/9)\gamma_C\gamma_H\beta^2(^3\Delta E)^{-1}S_C^2(0)S_H^2(0)P_{s_Cs_H}{}^2 \quad (8)$$

where $P_{s_Cs_H}$ denotes the bond order between the valence s orbital of C atom and that of H atom. Equation (6) or (8) indicates that the coupling constant is approximately proportional to $\pi_{s_Cs_H}$ or $P^2{}_{s_Cs_H}$. Table VI lists $\pi_{s_Cs_H}$ and $P^2{}_{s_Cs_H}$ estimated by the CNDO/2 calculations and the observed one-bond ^{13}C–^1H coupling constants ($^1J_{C-H}$). The examination of Table VI reveals a good correlation between the observed $^1J_{C-H}$ and $\pi_{s_Cs_H}$ or $P^2{}_{s_Cs_H}$. The constants in Eq. (6)

TABLE VI. $\pi_{s_Cs_H}$ and $P^2{}_{s_Cs_H}$ estimated by CNDO/2 Calculations and Observed $^1J_{C-H}$

Position	$\pi_{s_Cs_H}$ ($\times 10^{-2}$)	$P^2{}_{s_Cs_H}$	$^1J_{C-H}$ (Hz)
4	−0.80	0.313	173
N–CH_3	−0.60	0.252	136
C–CH_3	−0.56	0.242	127
2′, 6′	−0.67	0.275	161
3′, 5′	−0.68	0.276	155
4′	−0.68	0.275	159

and (8) were evaluated by fitting the equations to the data in Table VI. The results are given in Eq. (9) and (10).

$$^1J_{C-H} = -22815\pi_{s_Cs_H} \quad (9)$$

$$^1J_{C-H} = 559.1P^2{}_{s_Cs_H} \quad (10)$$

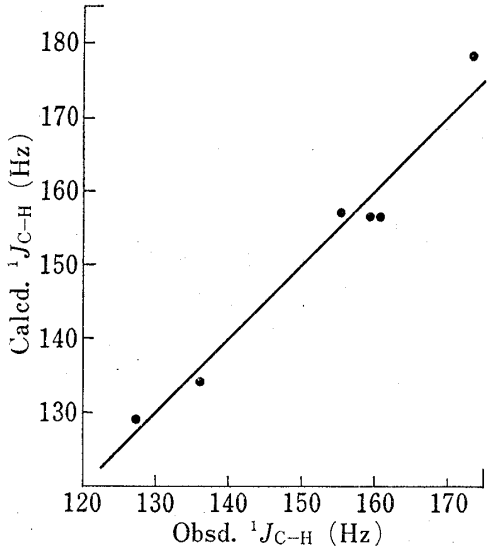

Fig. 6. Plot of Observed *versus* Predicted $^1J_{C-H}$ by Eq. (9) ($r=0.953$)

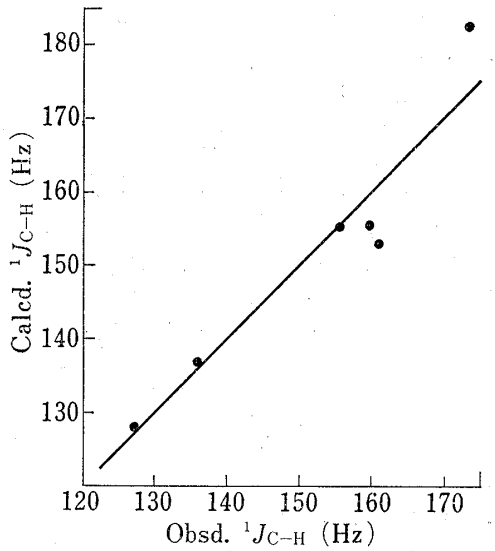

Fig. 7. Plot of Observed *versus* Calculated $^1J_{C-H}$ by Eq. (10) ($r=0.952$)

Table VII. Analysis of sp^3-Carbon Chemical Shifts
(Example: Aminopropylon)

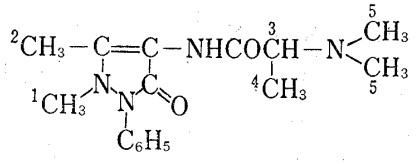

Position	α		β			γ			δ	$\delta_c(i)_{obsd.}$
	C	N	C	N	O	C	N	O	C	
1		1	1	1		4			4	35.9
2	1		1	1		2	2		3	11.1
3	2	1	2	1	1	1			2	62.8
4	1		1	1		2	1	1	1	12.4
5		1	2			2				40.4

The values estimated by Eq. (9) or (10) are plotted against the observed values in Fig. 6 or 7, respectively. The correlation coefficient (r) is 0.953 for Eq. (9) and 0.952 for Eq. (10).

Additive Law

Additive equations were calculated on chemical shifts of the sp^3-carbon, adding chemical shift data on forty-eight barbituric acid derivatives previously reported.[2,6,8] The analyzing procedure in the case of aminopropylon is, for example, shown in Table VII. Namely, the first position from the sp^3-carbon (i) is termed the α-position, the second β, the third γ and so on. The numbers of the atoms belong to the α, β, γ and δ positions are counted. The atoms, which overlap in two positions owing to containing the ring on counting for the number of the atoms belong to each position, were counted twice in the corresponding positions. In the next place, assuming an equation $\delta_c(i)=\text{const.}+\sum_{j,k}B_{ijk}n_{ijk}$ can apply in the chemical shifts of the sp^3-carbon, an additive equation was estimated using the least-square method. The result is given in Eq. (11),

$$\delta_c(i) = 5.32 + \sum_{j,k} B_{ijk}n_{ijk} \qquad (11)$$

where B_{ijk} is the additive chemical shift parameter of the atom (i, j, k), n_{ijk} is the number of the atoms belong to the atom (i, j, k), the suffix j denotes the kind of the atom, that is, C, N, or O, and the suffix k denotes the position from the sp^3-carbon (i), that is, α, β, γ, or δ, respectively. Table VIII gives the values of the additive parameter B_{ijk}. It can be seen that both α- and β-atoms cause downfield shifts, but that the γ-atoms produce upfield shifts. The values estimated by Eq. (11) are plotted against the observed values in Fig. 8. The correlation coefficient (s) is 0.980 and the standard deviation (s) is 3.432.

Table VIII. Additive Parameter Values and 95% Confidence Limits

k	j		
	C	N	O
α	5.27±0.80	21.75±1.64	
β	7.12±0.69	2.95±1.65	8.25±1.79
γ	−1.48±0.54	−1.59±1.35	−0.89±1.21
δ	−0.05±0.48		

8) J. Okada and T. Esaki, *Yakugaku Zasshi*, 93, 1014 (1973).

TABLE IX. Examples of Steric Effects

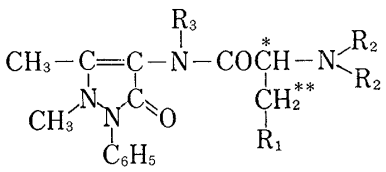

No.1—No.8

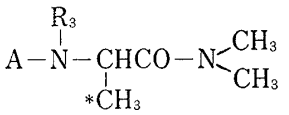

No.9—No.10

No.	R_1	R_2	R_3	*	$\Delta(\gamma)$	**	$\Delta(\delta)$ (ppm)
1	H	CH_3	H	62.8	−4.5	12.4	−1.9
2	H	CH_3	CH_3	58.3		10.5	
3	H	C_2H_5	H	58.6	−4.3	10.4	−0.9
4	H	C_2H_5	CH_3	54.3		9.5	
5	CH_3	CH_3	H	68.8	−4.3	21.7	−4.1
6	CH_3	CH_3	CH_3	64.5		17.6	
7	C_2H_5	CH_3	H	67.1	−4.3	31.1	−4.9
8	C_2H_5	CH_3	CH_3	62.8		26.2	
9	—	—	H	19.0	−4.5		
10	—	—	CH_3	14.5			
	From Eq. (11)				−1.48±0.54		−0.05±0.48

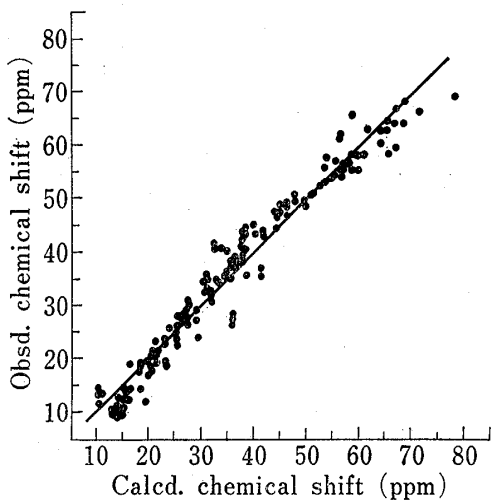

Fig.8 . Plot of Obsd. *versus* Calcd. Chemical Shift of sp^3-Carbon (r=0.980, s=3.432)

Now, an additive equation considering the bond character of the carbon atoms, that is, the single bond or the double bond, was estimated in a similar manner. The correlation coefficient (r) is 0.980 and the standard deviation(s) is 3.450 in this case. Obviously, the difference of these two cases cannot be regarded as significant.

Incidentally, Table IX presents some examples of the steric effects.[9] According to Table IX, the corresponding carbon chemical shifts appear at higher fields than those expected from Eq. (11) when the methyl radical attachs to the substituent position R_3. These phenomena can be accounted for by the effects of steric compression which are caused by attachment of the methyl radical to the R_3 position.

Structure-Activity Relationship

The activity of the drug is, in general, expressed by Eq. (12) in the Hansch analysis.

$$\log(1/C) = -k_1\pi^2 + k_2\pi + k_3\sigma + k_4E_s + k_5 \qquad (12)$$

where C is the applied concentration (dose), π is the substituent constant defined as: $\pi = \log(P_X/P_H)$ where P_H is the partition coefficient for a parent compound and P_X is that for a derivative, σ is Hammett's constant and E_s is Taft's steric parameter. The physico-chemical interpretations of these parameters are as follows: π^2 and π represent the transport process and π, σ and E_s represent the intrinsic activity of the drug at the active site, where π denotes the hydrophobic, σ the electronic and E_s the steric contribution. Previously, the authors replaced the electronic parameter σ in Eq. (12) by a quantity A expressed by the value related to the chemical shift of the carbon of the so-called biological active center. According to

9) D.M. Grant and B.V. Cheney, *J. Am. Chem. Soc.*, **89**, 5315 (1967).

TABLE X. Hansch Analysis of Antipyrine Derivatives

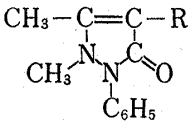

No.	R	π	A	P_E	P_r	$\log(1/C)_{ED_{50}}$ obsd.	$\log(1/C)_{ED_{50}}$ calcd.	$\log(1/C)_{LD_{50}}$ obsd.	$\log(1/C)_{LD_{50}}$ calcd.
1	H	0	0	0	0	—	—	2.340	2.628
2	$N(CH_3)_2$	0.59	25.1	13.2	113	3.303	3.254	2.902	2.862
3	$N(CH_3)CH_2SO_3Na$	0.11	21.0	24.5	222	—	—	2.213	2.153
4	$NHCOCH_2N(CH_3)_2$	−0.75	10.6	26.0	235	—	—	2.138	2.380
5	$NHCOCH(CH_3)N(CH_3)_2$	−0.43	10.5	30.7	275	3.401	3.557	2.420	2.534
6	$N(CH_3)COCH(CH_3)N(CH_3)_2$	−1.18	15.8	35.6	315	3.178	3.298	2.393	2.913
7	$N(CH_3)COCH(CH_3)N(C_2H_5)_2$	−0.62	16.4	44.8	395	3.745	3.611	2.745	2.884
8	$N(CH_3)COCH(C_2H_5)N(CH_3)_2$	−0.73	15.9	40.2	355	3.644	3.570	2.624	2.772
9	$NHCH(CH_3)CON(CH_3)_2$	−0.03	19.1	30.7	275	3.420	3.608	2.863	2.387
10	$N(CH_3)CH(CH_3)CON(CH_3)_2$	0.31	22.5	35.6	315	3.527	3.465	2.701	2.987
11	$COCH_2N(CH_3)_2$	−1.33	6.9	22.4	202	—	—	3.222	2.922
12	$COCH(CH_3)N(CH_3)_2$	−1.16	7.3	27.1	242	3.173	3.197	2.983	2.862
13	$COCH(CH_3)N(C_2H_5)_2$	−0.95	7.2	36.3	322	—	—	3.126	3.003
14	$COCH(C_2H_5)N(CH_3)_2$	−0.62	7.9	31.7	282	—	—	3.099	2.699
15	$COCH(C_2H_5)N(C_2H_5)_2$	−0.40	7.7	40.9	362	3.620	3.519	3.232	3.132
16	$COCH(iso\text{-}C_3H_7)N(CH_3)_2$	−0.04	9.5	36.3	322	3.409	3.480	2.897	3.036
17	$NHCONH_2$	−1.30	7.1	11.7	115	3.095	3.070	2.011	2.237
18	$NHCONHCOCH_2N(CH_3)_2$	−0.69	9.2	34.3	316	3.623	3.491	2.172	2.205
19	$NHCONHCOCH(CH_3)N(CH_3)_2$	−0.26	9.5	38.9	356	3.530	3.535	2.061	2.426

Hansch, *et al.*,[10] the steric parameter E_s in Eq. (12) can be also replaced by a quantity P_E related to the molar refraction (MR). Therefore, Eq. (12) can be rewritten to Eq. (13).

$$\log(1/C) = -k_1\pi^2 + k_2\pi + k_3A + k_4P_E + k_5 \quad (13)$$

In this paper, we have estimated the Hansch equations on the analgesic activities (ED_{50}) and the toxities (LD_{50}) of the antipyrine derivatives by using Eq. (13). The data used in these analyses are collected in Table X, where the log $(1/C)$ (C: mole/kg) values were calculated from the ED_{50} or the LD_{50} values with mouses as the experimental animals, extracted from the literature,[11] and the π, A and P_E values are calculated by Eq. (14).

$$\left.\begin{array}{ll} \pi = \log P_R - \log P_H & \log P_H = 0.38 \\ A = \delta_c(4)_R - \delta_c(4)_H & \delta_c(4)_H = 96.4\ (\text{ppm}) \\ P_E = MR_R - MR_H & \end{array}\right\} \quad (14)$$

where P is the observed partition coefficient which was determined in an n-octanol-water system, δ_c (4) is the observed chemical shift at C-4 and MR is the value estimated by the atomic refractions listed in Table XI, using the additive property. Equations (15)—(17) resulted from the least-squares fits with the data on ED_{50};

$$ED_{50}: \log(1/C) = -0.440\pi^2 - 0.245\pi + 3.549 \quad (15)$$
$$(r=0.804,\ s=0.133)$$
$$\log(1/C) = -0.529\pi^2 - 0.409\pi + 0.137\times10^{-1}A + 3.335 \quad (16)$$
$$(r=0.850,\ s=0.124)$$

10) C. Hansch, A. Leo, S.H. Unger, K.H. Kim, D. Nikaitani, and E.J. Lien, *J. Med. Chem.*, **16**, 1207 (1973).
11) *a*) K. Ogiu, H. Fujimura, M. Matsumura, T. Ueshima, T. Takahashi, and S. Senda, *Yakugaku Zasshi*, **73**, 437 (1953); *b*) T. Takahashi and K. Kanematsu, *ibid.*, **78**, 787 (1958); *c*) *Idem*, *ibid.*, **79**, 172 (1959); *d*) K. Ogiu, H. Fujimura, M. Matsumura, and T. Ueshima, *Nippon Yakurigaku Zasshi*, **49**, 289 (1953); *e*) H. Fujimura and K. Ohata, *Yakugaku Kenkyu*, **31**, 140 (1959).

$$\log(1/C) = -0.344\pi^2 - 0.225\pi + 0.885\times10^{-2}A + 0.654\times10^{-2}P_E + 3.179 \quad (17)$$
$$(r=0.866,\ s=0.125)$$

The F-test reveals that the A-term in Eq. (16) is significant at the 25% significant level but the P_E-term in Eq. (17) is not significant at the 25% significant level, namely the correlation coefficient "r" of Eq. (16) ($r=0.850$) is greater than that of Eq. (15) ($r=0.804$) but "r" of Eq. (17) ($r=0.866$) is nearly equal to that of Eq. (16) ($r=0.850$).

By the way, Eq. (18) resulted from the data on LD_{50}.

$$\log(1/C) = 1.039\pi^2 + 1.263\pi - 0.434\times10^{-1}A + 0.312\times10^{-1}P_E + 2.316 \quad (18)$$
$$(r=0.553,\ s=0.388)$$

But the correlation obtained with Eq. (18) is so low that the calculated values cannot predict the observed toxities exactly. Therefore, Eq. (19) was obtained, adding the parameter P_r expressed as: $P_r=PC_R-PC_H$ where PC is the parachor value estimated by the atomic parachor in Table XII using the additive property, in order to improve this defect.

$$\log(1/C) = 0.868\pi^2 + 1.009\pi - 0.455\times10^{-1}A + 0.4391P_E - 0.4663\times10^{-1}P_r + 2.628 \quad (19)$$
$$(r=0.771,\ s=0.313)$$

The F-test reveals that the P_r-term in Eq. (19) is significant at the 2.5% significant level, namely the correlation coefficient "r" of Eq. (19) ($r=0.771$) is greater than that of Eq. (18) ($r=0.553$).

Table XI. Atomic Refraction (D-Ray)

Atom		AR
C		2.418
H		1.100
O (C=O)		2.219
Double Bond (C=C)		1.733
N	aliphatic primary	2.322
N	aliphatic secondary	2.499
N	aliphatic tertiary	2.840

Table XII. Atomic Parachor[a)]

Atom	AP
C	9.0
H	15.5
O	19.8
N	17.5
S	49.1
Double Bond	19.9

a) O.R. Quayle, *Chem. Rev*, **53**, 443 (1953).

The calculated values in Table X are those obtained using Eq. (16) for ED_{50} and Eq. (19) for LD_{50}

Experimental

Preparation of Compounds——The 4-substituted antipyrine derivatives, whose ^{13}C NMR spectra were measured, were prepared by the methods given in the literature.[11b,12-16)]

12) F. Kusuda, "Iyakuhin Kaihatsu Kiso Koza VIII, Shin-iyakuhin no Goseiho (Jo)," ed. by K. Tsuda and H. Nogami, Chijin Syokan, Tokyo, 1972, pp. 141—152.
13) *a*) R. Kondo and N. Kikuchi, "Jikken Yakuhin Goseiho Zenshu," Vol. II, ed. by Hygienic Laboratory in Ministry of Public Welfare, Sasaki Tosho, Tokyo, 1948, p. 241; *b*) R. Kondo and S. Zenki, *ibid.*, p. 245; *c*) K. Shinosaki, *ibid.*, p. 256; *d*) *Idem*, *ibid.*, p. 272.
14) S. Yamaguchi, "Jikken Uki Kagaku," revised ed., Nankodo, Tokyo, 1942, pp. 81—82.
15) W.E. Weaver and W.M. Whaley, *J. Am. Chem. Soc.*, **69**, 1144 (1947).
16) *a*) Y. Sawa, *Yakugaku Zasshi*, **57**, 953 (1937); *b*) T. Takahashi and S. Senda, *ibid.*, **72**, 614 (1952); *c*) T. Takahashi, J. Okada, and M. Hori, *ibid.*, **75**, 1431 (1955); *d*) T. Takahashi, M. Hori, and K. Kanematsu, *ibid.*, **76**, 568 (1956); *e*) T. Takahashi, J. Okada, M. Hori, A. Kato, K. Kanematsu, and Y. Yamamoto, *ibid.*, **76**, 1180 (1956); *f*) T. Takahashi and Y. Matsuo, *ibid.*, **80**, 171 (1960).

Measurements of ^{13}C NMR Spectra——^{13}C NMR spectra of the compounds except antipyrine-Pr(fod)$_3$ complexes were determined on a Hitachi R-26 PFT spectrometer operating at 10 MHz using 10-mm o.d. tubes at 35° in the ^1H-noise decoupled state. The off-resonance and the proton undecoupled spectra of antipyrine (No. 25) were also measured. A small amount of tetramethylsilane (TMS) was added as an internal reference, but a capillary tube containing TMS was used as an external reference in the cases of the measurements of compounds No. 21, 22, 29, and 30 (see Table I). A capillary tube containing D_2O was added to provide a lock signal. The sample solutions were prepared in the concentration range of 0.3 to 1.0M. The experiments which were carried out to check for the concentration effect in dimethyl sulfoxide (DMSO) showed that the concentration change, within the range of 0.3—1.0 M, had no apparent effect on the chemical shifts. The other PFT NMR experimental conditions were as follows; pulse interval 4 sec, pulse angle 45°, sampling period 0.2 sec, pulse location carbon disulfide (CS_2), 512-*ca.* 15000 scans accumulated in 2048 channel signal averager. The estimated precision is ± 1 ppm for the shieldings, and ± 10 Hz for the coupling constants.

^{13}C NMR spectra of antipyrine-Pr(fod)$_3$ complexes were determined on a NEVA NV-21 PFT spectrometer operating at 22.6 MHz using 8-mm o.d. tubes in the ^1H-noise-decoupled state. The sample solution, in which TMS was added as an internal reference, was prepared in the concentration of *ca.* 1.0 M deuteriochloroform ($CDCl_3$).

Measurements of Partition Coefficients——Commercially available *n*-octanol (first or special grade), which was purified by distillation, was used for organic phase, and the Sørensen's phosphate buffer, pH 7.4, for water phase. The partitioning experiments were carried out as follows: a mixture of 15 ml portions of *n*-octanol and 40 ml portions of the buffer, in which 5 to 20 mg of the sample (10^{-4}—10^{-3} M) was dissolved, was placed into a stirring vessel, maintained at 37° in a thermostat, followed by stirring at 600 rpm for 30 minutes in order to obtain an equibrium distribution of the solute. The analysis of the concentrations of the partitioned substances in both phases were made by ultraviolet spectroscopy using a Shimazu QV-50 spectrometer. The partition coefficient was calculated as $P = C_{\text{octanol}}/C_{H_2O}$ by ignoring association and dissociation of the solute in both phases. The average of the partition coefficients, which were measured 3—5 times by the above-mentioned manner, was adopted the observed value.

Acknowledgement The authors wish to express their sincere thanks to Miss M. Sugiura of Kobe Woman's Pharmaceutical College for her assistance in measuring some of the ^{13}C NMR spectra, and also to J. Mori, Bachelor of Pharmacy, for her assistance in the experimental work.